Available online at www.sciencedirect.com
ScienceDirect
Journal of the European Ceramic Society 28 (2008) 2233–2238
www.elsevier.com/locate/jeurceramsoc

Synthesis of bismuth ferrite lead titanate nano-powders and ceramics using chemical co-precipitation

Tim P. Comyn *, David F. Kanguwe, Jingyan He, Andrew P. Brown

Institute for Materials Research, University of Leeds, Leeds LS2 9JT, UK

Received 26 November 2007; received in revised form 12 February 2008; accepted 29 February 2008
Available online 5 May 2008

Abstract

The high temperature ferroelectric material $BiFeO_3$–$PbTiO_3$ was fabricated via chemical co-precipitation using $Bi(NO_3)_3{\cdot}(H_2O)_5$, $Fe(NO_3)_3{\cdot}(H_2O)_9$, $Pb(NO_3)_2$ and TiI_4 as precursors. The prepared composition was close to the target composition, as determined by XRF and EDX. Calcination at 800 °C yielded a single phase powder, with a primary particle size in the range 20–75 nm, and were single crystallites, as determined using TEM. Pellets fabricated from the powder were sintered to a maximum density at 950 °C, some 65–75 °C lower than using a conventional mixed oxide route, and had a density of 95% of theoretical. The sintered pellets had a relative permittivity of 190 compared to 280 for conventionally prepared materials.

Keywords: Powders—chemical preparation; Electron microscopy; X-ray methods; Dielectric properties; $BiFeO_3$–$PbTiO_3$

1. Introduction

Materials based on the $(BiFeO_3)_x$–$(PbTiO_3)_{1-x}$ (BFPT) system have considerable potential for use in high temperature piezoelectric and ferroelectric applications, displaying both a morphotropic phase boundary (MPB) and a high transition temperature;[1] at the MPB which occurs at $x = 0.70$,[2] the temperature of the ferroelectric–paraelectric phase transition is at 632 °C. An extremely high tetragonality of around 19%[3] in conjunction with suitability for single crystal formation[4] lends exciting potential for the development of enormous strain during rhombohedral–tetragonal phase switching, over a considerable temperature range.

The fabrication of BFPT has been reported using a number of preparative routes including conventional mixed oxide synthesis,[5,6] mechanical activation,[7] sol–gel[8] and flux-growth of single crystals. The materials reported here have been fabricated using a novel chemical precipitation technique aimed at the generation of nano-particles. Fine particles are well known to reduce the sintering temperature[9] and the level of porosity of ceramics.[10] Both of these effects are extremely important in this class of material in order to reduce the effect of PbO and Bi_2O_3 volatilisation, and increase both the dielectric and mechanical strength of the material so as to withstand the high electrical and physical stresses that may be imposed during poling and actuation. Lowering of the sintering temperature without resorting to chemical sintering aids is also of importance with regard to the fabrication of multi-layers incorporating non-precious metal electrodes.

2. Experimental procedure

In order to fabricate BFPT, $Bi(NO_3)_3{\cdot}(H_2O)_5$ (98+%), $Fe(NO_3)_3{\cdot}(H_2O)_9$ (98+%), $Pb(NO_3)_2$ (99+%) and TiI_4 (98%) powders were used as precursors (Aldrich, UK). TiI_4 was used as an alternative to both $TiCl_4$ and $Ti(NO_3)_4$ as the chloride is extremely air sensitive, and the nitrate is prohibitively expensive. In order to determine the yields, each of the precursors was precipitated individually from 0.5 M solutions in de-ionised water using ammonium hydroxide. The final suspension was continually washed until a pH of 7 was obtained. Each of the powders was filtered, dried, weighed and analysed by X-ray diffraction (XRD) to determine the phases formed. Differential thermal analysis (DTA, PerkinElmer, DTA 7, Boston, USA) of the powders was performed and then, as required, the powders subjected to various calcination schedules.

* Corresponding author. Tel.: +44 113 3432540; fax: +44 113 3432384.
E-mail address: t.p.comyn@leeds.ac.uk (T.P. Comyn).

0955-2219/$ – see front matter © 2008 Elsevier Ltd. All rights reserved.
doi:10.1016/j.jeurceramsoc.2008.02.013

From the yields determined, appropriate quantities of the precursors were weighed and dissolved into distilled water in order to fabricate the MPB composition 0.7 ($BiFeO_3$)–0.3 ($PbTiO_3$) via phase co-precipitation. These were precipitated as above for the individual precursors and again the suspension pH adjusted to 7. A range of calcination temperatures from 600 to 800 °C was employed, and the progress monitored using XRD (PANalytical X'Pert MPD system, Philips, Netherlands), SEM (Leo Gemini 1530 FEG-SEM, Cambridge, UK), and EDX (energy dispersive X-ray, Inca, Oxford Instruments, UK). The chemical composition of the material fabricated using the most suitable processing route was also verified using XRF (X-ray fluorescence spectroscopy, London and Scandinavian Metallurgical, Rotherham, UK).

10 mm pellets were uniaxially pressed at 100 MPa directly from the calcined powder with no intermediate milling or binder addition; it was the intention of this work to exclude any effect of milling. The pellets were sintered at a range of temperatures, and the densities recorded; in all instances a dwell time of 120 and 30 min was employed for calcination and sintering, respectively. Electrodes were applied using air-drying silver paint (Agar Scientific, Stansted, UK), and the relative permittivity measured at 1 kHz using an impedance analyser (Agilent 4294A). In order to perform chemical analysis on the pellets, the surface was polished to 1 μm using diamond paste. XRD was performed on the polished surfaces after annealing at 700 °C for 5 min in air, then cooling at 25 °C/h to room temperature, in order to alleviate surface stress.

TEM samples were prepared by drop-casting powders onto standard holey carbon support films (Agar Scientific, UK). TEM was performed on a FEI CM200 FEG-TEM (Philips, Netherlands) with EDX (Oxford Instruments, UK).

3. Results

3.1. Precursor yield and phase study

DTA analyses of the precursors after precipitation showed a range of features indicating the temperatures of physical and chemical reactions. The highest temperature of an exothermic or endothermic peak (below the melting points of Bi_2O_3 and PbO at 813 and 871 °C, respectively) was taken as a guide for the minimum required calcination temperature of each component. The DTA reaction temperatures, the calcination temperatures used, along with the yield of powder fabricated are shown in Table 1. XRD analyses of the powders after calcination show that, with the exception of the titanium precursor, pure oxides were formed at the calcination temperatures as prescribed by DTA. In the case of the titanium precursor calcined at 450 °C, a second phase was present in addition to TiO_2 which we were unable to identify using the ICDD (The International Centre for Diffraction Data) database; SEM–EDX of this powder revealed the presence of iodine. Increasing the calcination temperature to 600 °C drove off the remaining iodine and resulted in the formation of phase pure TiO_2.

Table 1
Maximum temperature of DTA feature (highest temperature of physical or chemical change bar melting), calcination temperature used and yield of oxide recovered

Precursor	Maximum temperature of DTA feature (°C)	Calcination temperature (°C)	Yield (%)
$Bi(NO_3)_3{\cdot}(H_2O)_5$	572	600	96.4
$Fe(NO_3)_3{\cdot}(H_2O)_9$	395	450	99.7
$Pb(NO_3)_2$	545	600	90.0
TiI_4	430	600	95.0

3.2. Co-precipitation of BFPT

Appropriate quantities of the precursors in order to fabricate $(BiFeO_3)_{0.7}$–$(PbTiO_3)_{0.3}$ were co-precipitated, taking into account the yield values shown in Table 1. Calcination of the precipitate at 600 °C yielded a mixed phase powder, as determined by XRD (Fig. 1). Increasing the calcination temperature to 800 °C produced an essentially single phase powder (there is less than 2% residual Bi_2O_3 as determined by quantitative phase analysis), with cubic symmetry and with $a = 3.964$ Å. The calcination temperature of 800 °C is considerably lower than that required to prepare single phase material from conventional mixed oxide powders of 925 °C.[6]

The reason for the presence of cubic symmetry rather than rhombohedral or tetragonal may be as a result of the fine particle size; such phenomena have been observed in $BaTiO_3$.[11,12] DTA was used in order to search for a phase change, which may be indicative of the ferroelectric–paraelectric transition; no such feature was apparent lending more support to the fact that the phase produced was cubic, and therefore paraelectric. At a calcination temperature of 700 °C, XRD indicated a mixture of the intended phase and $PbBiO_2I$. SEM–EDX of the powders calcined at different temperatures revealed the existence of residual iodine (Table 2). Observation of the powders using SEM (Fig. 2) shows a reduction in particle size with increasing calcination temperature, perhaps indicating the volatilisation of the iodine-rich phase. As can be seen from Fig. 2(b), the final particle size is extremely fine, ranging from 20 to 75 nm. Compositional analysis using EDX and XRF indicate that the powder

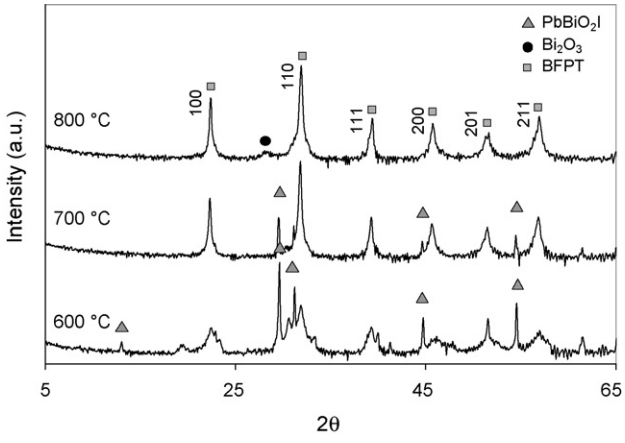

Fig. 1. XRD of co-precipitated powder calcined at 600, 700 and 800 °C.

Table 2
Iodine content of synthesized powder, prior to calcination and after calcination at a range of temperatures estimated by semi-quantitative analysis of SEM–EDX spectra

Calcination temperature (°C)	Iodine content (wt.%)
Uncalcined	12.0
600	8.8
700	2.3
800	0.0

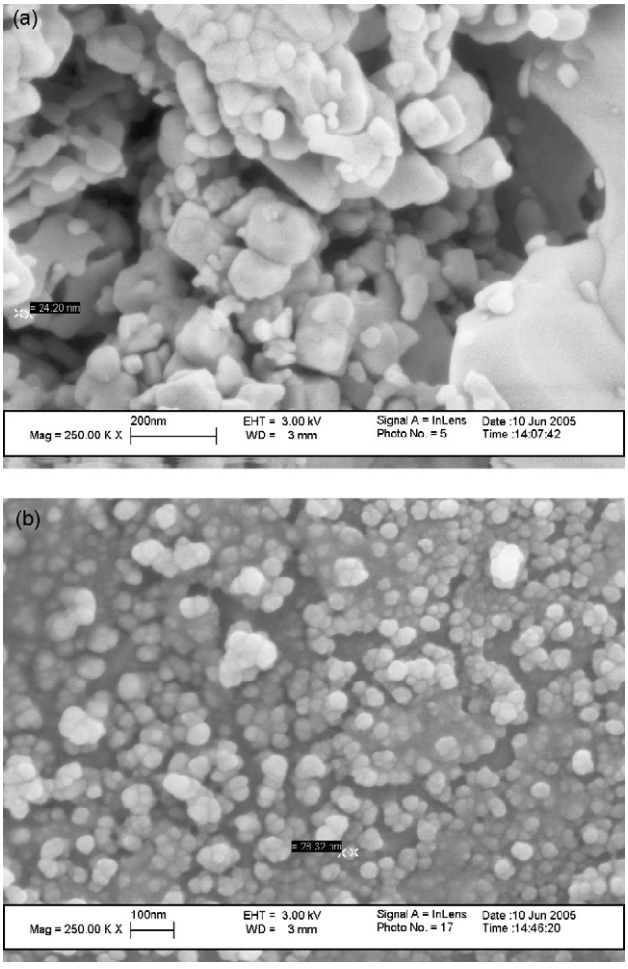

Fig. 2. SEM of precipitated powder after calcination at (a) 600 °C and (b) 800 °C. The particle size is clearly in the range 20–75 nm.

calcined at 800 °C is close to the target composition, as shown in Table 3. The data is normalised such that there are three oxygen atoms per unit cell; it is not possible to get a sensible value for the oxygen stoichiometry using either EDX or XRF. Both

Table 3
Target composition and actual composition fabricated as determined by semi-quantitative analysis of EDX and XRF

	Formulae
Target composition	$Bi_{0.70}Fe_{0.70}Pb_{0.30}Ti_{0.30}O_3$
Powder calcined at 800 °C (EDX)	$Bi_{0.72}Fe_{0.78}Pb_{0.31}Ti_{0.23}O_3$
Powder calcined at 800 °C (XRF)	$Bi_{0.70}Fe_{0.72}Pb_{0.34}Ti_{0.26}O_3$

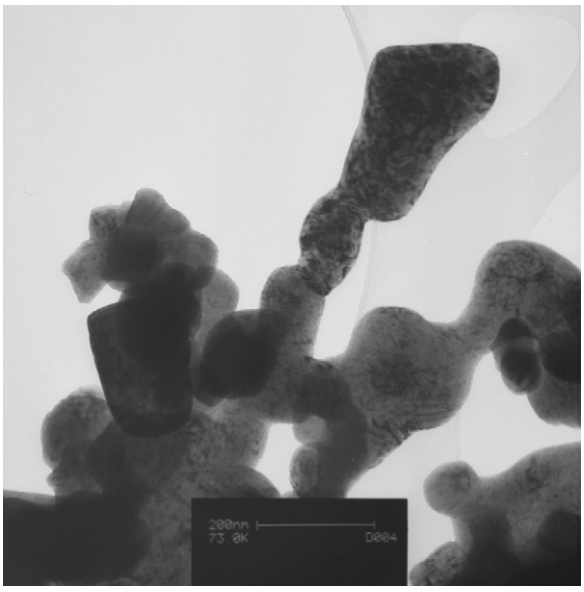

Fig. 3. TEM of co-precipitated powder calcined at 800 °C. The variable contrast within the particles can be assigned to high levels of strain.

analysis techniques suggest that the fabricated techniques are Ti deficient. Two possible reasons for the deviation from the desired composition are measurement error and changes to the yields during the reaction of multiple precursors. Measurement of Bi and Pb concentrations using EDX is extremely difficult as the energies are similar and there is considerable overlap.

3.3. TEM of calcined powders

TEM micrographs of the precipitated powder calcined at 800 °C are shown in Figs. 3 and 4. It can be seen that the particles are single crystallites, as indicated by the continuous lattice.

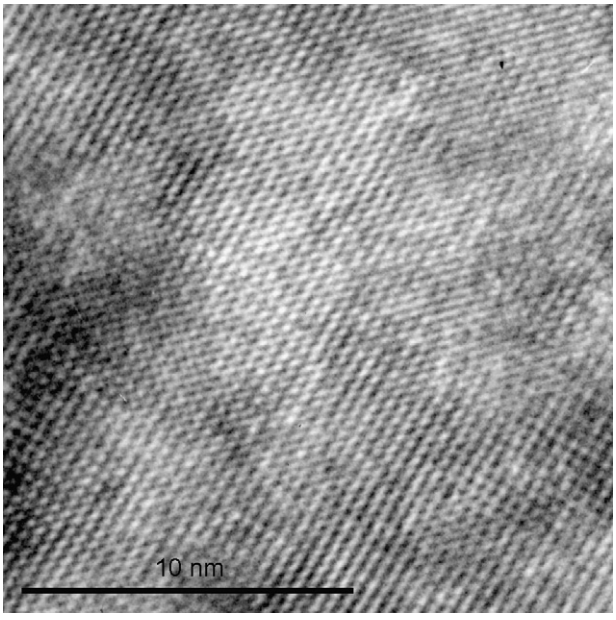

Fig. 4. TEM of co-precipitated powder calcined at 800 °C showing a continuous lattice. These lattice lines run throughout the grains shown in Figs. 2 and 3.

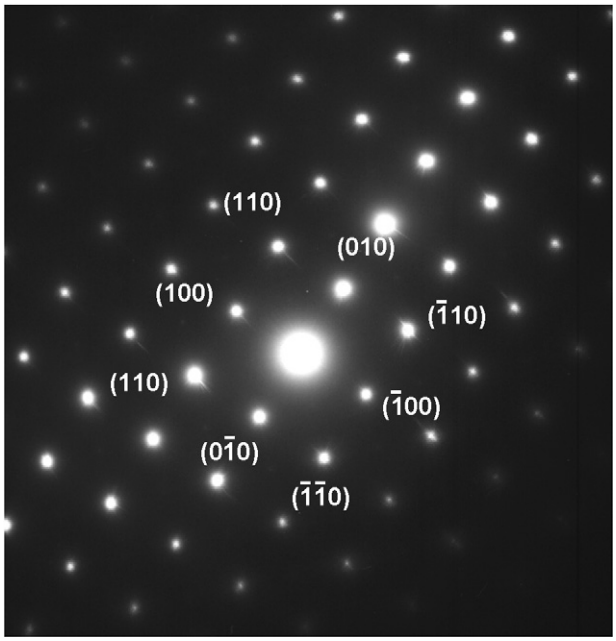

Fig. 5. Electron diffraction pattern for co-precipitated powder calcined at 800 °C. The pattern is indexed to a cubic symmetry, with $a = 4.38$ Å with zone axis 001.

Electron diffraction of the particles (Fig. 5) indicates again a single phase with a cubic structure, but with a lattice parameter $a = 4.38$ Å, 10% larger than observed using XRD. This is within an acceptable error range due to the calibrated camera constant in the TEM used. Large variations in contrast are visible in the images. EDX suggests that these variations are not as a consequence of local variation in composition but rather stress, suggesting that they are a form of strain contrast. To this end, an analysis of XRD peak broadening was carried out.

Eq. (1) is a modified Scherrer relationship where β_t is the total peak breadth (full width half maximum), λ the X-ray wavelength, d the coherence length (taken to be the particle size in this case, where the particles are single crystallites), θ the incident radiation or detector angle and ε the average strain. A plot of $\beta_t \cos\theta$ vs. $\sin\theta$ yields a slope $= 2\varepsilon$ and an intercept $= 0.9\lambda/d$.

$$\beta_t \cos\theta = \frac{0.9\lambda}{d} + 2\varepsilon \sin\theta \quad (1)$$

Eq. (1) indicates that the average strain is 1.0%, with a standard error of 0.013,[13] and a particle size of 60 nm, which is commensurate with the particle size observed using SEM and TEM of 20–75 nm. There are large errors, however, inherent with the calculation of particle size in a material which is highly strained, as errors in the gradient are grossly magnified in a calculation of the intercept; the standard error for the particle size leads to a range of 10.5 nm to ∞.

EDX at five separate locations within a crystal suggests that the composition is $Bi_{0.77}Fe_{0.85}Pb_{0.23}Ti_{0.19}O_3$, which is different to the values obtained using the SEM and XRF (Table 3). EDX using the TEM suggests that the Bi and Fe content are far higher than the intended composition. This may well be as a consequence of beam damage, or the fact that a much smaller area was sampled, that was not indicative of the comparatively large quantity of powder used for XRD.

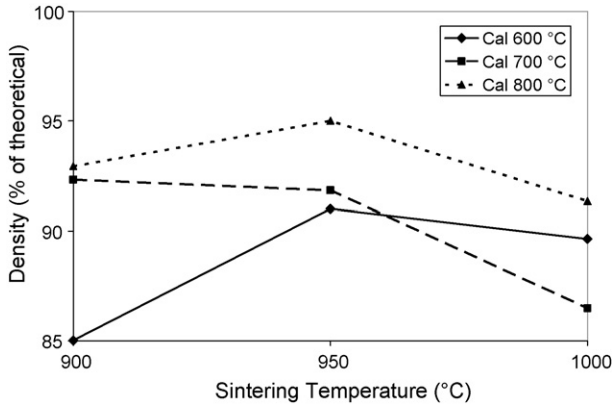

Fig. 6. Plot of the density as a percentage of theoretical for pellets prepared at a range of calcination and sintering temperatures. At 950 °C, the sintered density is greater than 95% of theoretical.

3.4. Sintering

The effect of sintering and calcination temperature on bulk density and relative permittivity are shown in Figs. 6 and 7, respectively. The theoretical density was calculated from XRD data for the densest pellet fabricated, whereby the powder was calcined at 800 °C and sintered at 950 °C. Fig. 6 shows a maximum density of greater than 95%, and a large dependence of the observed density on both calcination and sintering temperatures; in general, the higher calcination temperatures provide the highest sintered density, supposedly as a result of superior homogeneity, and a reduction in particle size. Note that the powders were not milled, and no binder was added after calcination; the powders were simply pressed and sintered; it was the intention of this work to ensure that milling was not employed at any point, so as not to influence particle size and morphology.

A permittivity analysis, as with the results from density measurements, indicates a general increase with calcination temperature, the pellet calcined at 600 °C and sintered

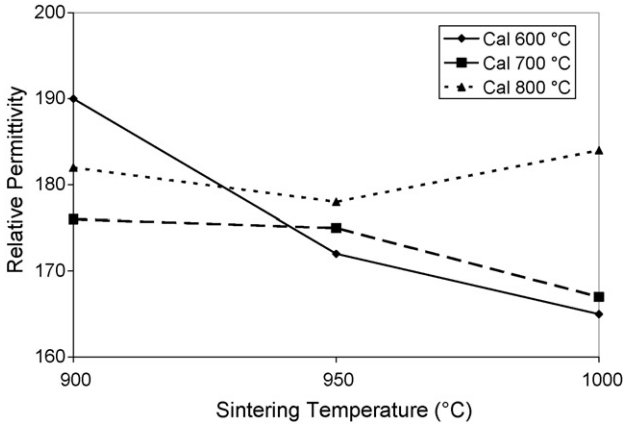

Fig. 7. Plot of the relative permittivity for pellets prepared at a range of calcination and sintering temperatures.

Table 4
Relative permittivity for range of compositions near the MPB in $(BiFeO_3)_x$–$(PbTiO_3)_{1-x}$

x	Relative permittivity
0.80	150
0.70	280
0.65	275

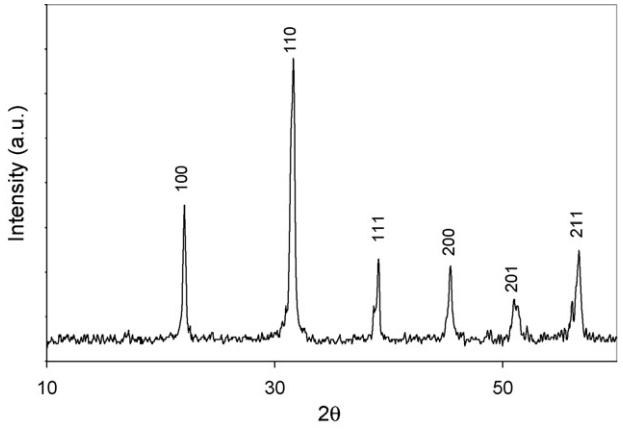

Fig. 8. XRD of pellet sintered at 950 °C, prepared from powder calcined at 800 °C. After polishing to a flat surface, the pellet was annealed at 700 °C to relieve stress and texturing. The material has a rhombohedral structure with $a = 3.996$ Å and $\alpha = 89.585°$.

at 900 °C being the exception. The relative permittivity of all the samples tested fall in the range 165–190. These values are slightly lower than that expected for conventionally prepared $(BiFeO_3)_{0.7}$–$(PbTiO_3)_{0.3}$, but reasonable taking into account the fact that the sintered materials are slightly off composition. Table 4 shows relative permittivity values measured for $(BiFeO_3)_x$–$(PbTiO_3)_{1-x}$ compositions near the MPB prepared using conventional mixed oxide synthesis, and it can be seen that a material within the range $x = 0.8$–0.7 would exhibit values similar to that observed. In lead zirconate titanate (PZT), a slight shift in composition near the MPB can introduce a large change in electrical properties.[14]

The XRD data for the pellet sintered at 950 °C from powder calcined at 800 °C is shown in Fig. 8. The figure shows that a rhombohedral structure is produced with $a = 3.996$ Å and $\alpha = 89.585°$, giving a unit cell volume of 63.803 Å^3 and in conjunction with the powder RMM of 315.759 g mol^{-1}, a theoretical density of 8.22 Mg m^{-3}. During sintering, the residual Bi_2O_3 that was apparent in the powder after calcination is no longer evident using XRD.

SEM of a fracture surface (Fig. 9) reveals a fine microstructure with an average particle of 1.1 μm, as determined by the linear intercept method. This is of the same order as is observed for BFPT sintered using conventional mixed oxide synthesis.

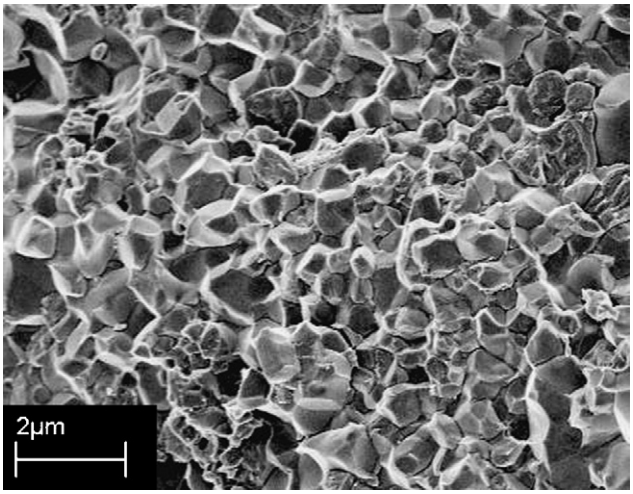

Fig. 9. SEM of fracture surface of pellet calcined at 800 °C and sintered at 950 °C showing an average particle size of 1.1 μm, as determined by the linear intercept method.

4. Conclusions

Perovskite BFPT was synthesized using chemical co-precipitation employing $Bi(NO_3)_3{\cdot}(H_2O)_5$, $Fe(NO_3)_3{\cdot}(H_2O)_9$,$Pb(NO_3)_2$ and TiI_4 as precursors. The composition and phase purity of the precipitated powders were verified using XRD, EDX (SEM and TEM) and XRF, and were found to deviate slightly from the intended composition. This could undoubtedly be remedied using further iterations of the starting concentrations. It was found that phase pure materials could be synthesized using a calcination temperature of 800 °C, some 125 °C lower than reported utilising conventional mixed oxide synthesis. A study of the powders using SEM and TEM showed a fine particle size of between 20 and 75 nm; each of these particles were single crystallites, as confirmed by electron diffraction. Analysis of the XRD peak breadth showed that the particles were highly strained, with an average value of 1%. This is consistent with the contrast variations observed in bright field TEM images.

Pellets were sintered from this powder to a density of 95% of theoretical, without further milling or the addition of binder. This density was achieved employing a sintering temperature of 950 °C, again lower than recorded via conventional mixed oxide synthesis by 65–75 °C. A maximum relative permittivity of 190 was recorded. The material has a rhombohedral structure with $a = 3.996$ Å and $\alpha = 89.585°$

The work reported here shows that chemical preparation can be used to prepare dense phase pure BFPT, using considerably lower calcination and sintering temperatures than previously reported. Such a reduction in processing temperatures will undoubtedly lead to less PbO and Bi_2O_3 volatilisation, and ultimately may provide materials which are suitable for multilayer fabrication using non-precious metal electrodes, without the use of sintering aids.

References

1. Fedulov, S. A., Ladyzhinskii, P. B., Pyatigorskaya, I. L. and Venevtsev, Y. N., Complete phase diagram of the $PbTiO_3$–$BiFeO_3$ system. *Soviet Phys.—Solid State*, 1964, **6**(2), 375–377.
2. Saw, C. K. and Kalnin, I. L., Diffraction studies of ferroelectric lead titanate bismuth ferrite ceramic. In *Proceedings of the 6th IEEE international symposium on applied ferroelectrics*, 1986, pp. 429–431.
3. Sai Sunder, V. V. S. S., Halliyal, A. and Umarji, A. M., Investigation of tetragonal distortion in the $PbTiO_3$–$BiFeO_3$ system by high temperature X-ray diffraction. *J. Mater. Res.*, 1995, **10**(5), 1301–1306.
4. Burnett, T. L., Comyn, T. P. and Bell, A. J., Flux growth of $BiFeO_3$–$PbTiO_3$ single crystals. *J. Cryst. Growth*, 2005, **285**, 156–161.
5. Woodward, D. I., Reaney, I. M., Eitel, R. E. and Randall, C. A., Crystal and domain structure of the $BiFeO_3$–$PbTiO_3$ solid solution. *J. Appl. Phys.*, 2003, **94**(5), 3313–3318.
6. Comyn, T. P., McBride, S. P. and Bell, A. J., Processing and electrical properties of $BiFeO_3$–$PbTiO_3$ ceramics. *Mater. Lett.*, 2004, **58**, 3844–3846.
7. Khan, M. A., Comyn, T. P. and Bell, A. J., Processing of nanoparticulate bismuth ferrite lead titanate (BFPT) through high-energy milling. *J. Am. Ceram. Soc.*, 2005, **88**(9), 2608–2610.
8. Sheng, H., Yue, Z., Gui, Z. and Li, L., Synthesis of $BiFeO_3$ $PbTiO_3$ powders by sol–gel auto-combustion process. *Key Eng. Mater.*, 2005, **280–283**, 609–612.
9. Maiwa, H., Kimura, O., Shoji, K. and Ochiai, H., Low temperature sintering of PZT ceramics without additives via an ordinary ceramic route. *J. Eur. Ceram. Soc.*, 2005, **25**, 2383–2385.
10. Duran, P. and Moure, C., Sintering at near theoretical density and properties of PZT ceramics chemically prepared. *J. Mater. Sci.*, 1985, **20**, 827–833.
11. Uchino, K., Sadanaga, E. and Hirose, T., Dependence of the crystal structure on particle size in barium titanate. *J. Am. Ceram. Soc.*, 1989, **72**(8), 1555–1558.
12. Chattopadhyay, S., Finite size effects in ferroelectric and antiferroelectric materials. *NanoStruct. Mater.*, 1997, **9**, 551–554.
13. Kelsall, R., Hamley, I. and Geoghegan, M., ed., *Nanoscale Science and Technology*. Wiley, Chichester, UK, 2005.
14. Jaffe, B., Cook, W. R. and Jaffe, H., *Piezoelectric Ceramics*. Academic Press, 1971.